MALAYSIAN JOURNAL OF ANALYTICAL SCIENCES

Journal homepage: https://mjas.analis.com.my/

Research Article

Preparation and characterization of modified rambutan peels for the removal of chromium(VI) and nickel(II) from aqueous solution: Environmental impact and optimization

Northaqifah Hasna Mohamed Khir[1,2], Nur Fatien Muhamad Salleh[1*], Noraini Abdul Ghafar[1], Nurasmat Mohd Shukri[1], and Rohayu Jusoh[3]

[1]School of Health Sciences, Universiti Sains Malaysia, Health Campus, 16150 Kubang Kerian, Kelantan, Malaysia
[2]Faculty of Applied Sciences, Universiti Teknologi MARA, Terengganu Branch, Bukit Besi Campus, 23200 Dungun, Terengganu, Malaysia
[3]Faculty of Chemical and Process Engineering Technology, Universiti Malaysia Pahang Al-Sultan Abdullah, Lebuh Persiaran Tun Khalil Yaakob, Gambang, Kuantan 26300, Pahang, Malaysia

[*]Corresponding author: nurfatiensalleh@usm.my

Received: 29 August 2024; Revised: 19 November 2024; Accepted: 3 December 2024; Published: 10 February 2025

Abstract
Recently, environmental remediation has focused on using cheap biosorbents to get rid of heavy metals. Agricultural wastes like rambutan peels are gaining more attention because they contain cellulose and hemicellulose and metal-binding capabilities. The natural presence of functional groups like hydroxyl (-OH) and methylene (-CH_2) in these peels facilitates metal biosorption, which can be further enhanced by acid treatment. This study evaluates the effectiveness of raw rambutan peels (RRP) and acid-treated rambutan peels (ATRP) in removing nickel (Ni(II)) and chromium (Cr(VI)) from aqueous solutions under varying conditions of contact time (30-150 minutes), pH (3-11), adsorbent dosage (0.5-4 g) and initial metal concentration (5-100 mg/L). Fourier-transform infrared (FTIR) analysis indicated an enhancement of O–H on the surface of ATRP following acid modification by stronger transmittance peaks at 3333.89 cm^{-1}, respectively. ATRP achieved 88.79% removal of Ni(II) with a 90-minute contact time at pH 7, and Cr(VI) at 70.11% with a 120-minute contact time at pH 5. Freundlich and Langmuir isotherm models were used to correlate sorption data. The result demonstrates that the Langmuir adsorption model fits best when compared to the Freundlich model with a coefficient of determination (R^2)=0.9698 and adsorption capacity (q_m) of 33.4448 mg/g for Cr(VI) and R^2 = 0.9699 with q_m of 416.6667 mg/g for Ni(II). Statistical analysis using the Mann-Whitney U Test confirmed significant differences in the biosorption efficiencies between RRP and ATRP in removing Cr(VI) (p = 0.009) and Ni(II) (p = 0.026), underscoring the superiority of the chemically modified biosorbent ATRP as a highly effective biosorbent for Cr(VI) and Ni(II) removal, offering a sustainable solution for environmental remediation.

Keywords: agricultural waste, acid treatment, biosorption, rambutan peels, chromium and nickel

Introduction

Heavy metal contamination in aquatic environments remains a critical challenge for environmental management, particularly in industrially active regions. Industrial discharges, including electroplating, leather tanning, and textile industries, primarily introduce heavy metals such as Cr(VI) and Ni(II) into water bodies [1]. In Malaysia, river pollution has intensified as industrial and domestic waste discharges continue unabated, affecting regions like Kedah, Pulau Pinang, Selangor, Kuala Lumpur, Johor, and Sarawak by 2024 [2-4]. Due to their high toxicity, non-biodegradability, and propensity to bioaccumulate, these metals pose significant threats to ecological and human health. Chronic exposure to these metals has been linked to a range of adverse health effects, including carcinogenesis, mutagenesis, and various organ dysfunctions, thereby necessitating effective and sustainable remediation strategies [5-8]. Therefore, the wastewater system plays a crucial role for industries that mostly discharge toxic heavy metals, ensuring compliance with the United States Environmental Protection Agency (USEPA) and

World Health Organisation (WHO) regulations to safeguard human health. The USEPA and WHO have established a guideline value for nickel in drinking water at 0.1 mg/L and 0.07 mg/L, respectively. Meanwhile, they also have recommended guideline values for total chromium in drinking water, which are 0.1 mg/L and 0.05 mg/L, respectively [9-10].

Traditional methods for heavy metal removal, such as chemical precipitation, ion exchange, and membrane filtration, often involve high operational costs, generate secondary pollution, and are difficult to implement in large-scale or resource-constrained settings [11-13]. These challenges have catalysed a shift towards exploring alternative, environmentally sustainable materials for water treatment. Agricultural wastes, characterised by their abundance, biodegradability, and lignocellulosic composition, have emerged as promising candidates for biosorption, offering an economically viable and ecologically friendly option [13-15].

The application of agricultural waste in environmental remediation aligns with the United Nations Sustainable Development Goals (SDGs), which provide a global blueprint for addressing key challenges in sustainability, resource management, and environmental protection. Utilising agricultural waste for environmental remediation correlates with several SDGs, specifically SDG6 for clean water and sanitation, SDG12 for sustainable consumption and production, and SDG14 for life below water [16]. Prior studies have demonstrated the effectiveness of several agricultural wastes, specifically fruit peels such as banana peels, orange peels, pomegranate peels, potato peels, and coconut husks, in removing heavy metals from water-based solutions [17-29]. By transforming agricultural waste into efficient biosorbents for water purification, this approach addresses water purification, promotes a circular economy, mitigates environmental pollution, and repurposes waste into valuable resources that support the essential sustainability objectives [14,15,17,18].

This study utilised *Nephelium lappaceum L.*, the primary rambutan species grown in Malaysia, which holds significant promise as a biosorbent. Malaysia's rambutan production reached 52,096.89 metric tonnes, with 37,925.79 metric tonnes harvested in Peninsular Malaysia alone, as reported by the Department of Agriculture Malaysia in 2022 [30]. The peel of *Nephelium lappaceum L.* constitutes a substantial portion of the fruit's mass, ranging from 45.7% to 64.7% depending on cultivar and maturity [31, 32]. This translates to approximately 23,808 to 33,707 metric tonnes of rambutan peel generated annually. Such quantities highlight its potential as an abundant and sustainable resource for biosorbent production while also addressing waste management challenges. Repurposing this agricultural waste aligns with SDG12, promoting resource efficiency and environmental sustainability.

Despite their widespread availability, rambutan peels are notable for their rich chemical composition, characterised by high cellulose levels, hemicellulose, and lignin. These components provide a large surface area and abundant binding sites for heavy metal ions. Specifically, the presence of functional groups such as hydroxyl (-OH), methylene ($-CH_2$), and carboxyl (-COOH) within the peels is conducive to complexing with heavy metal ions, thus enhancing their potential for effective biosorption. The study's environmental scope is further justified by the increasing emphasis on converting agricultural waste into valuable resources, thereby reducing environmental pollution and contributing to circular economy principles. However, the presence of lignin, which blocks the active sites, can limit the efficiency of these functional groups in their native state. Thus, chemical modification through acid treatment can expose more active sites, leading to an enhanced capacity for binding metal ions, thereby increasing the biosorption capacity [30-32].

This study aims to explore the efficacy of rambutan peel for Cr(VI) and Ni(II) removal from aqueous solutions, focusing on evaluating the impact of acid treatment on biosorption efficiency. The research objectives include determining the optimal operational parameters of contact time, pH, adsorbent dosage, and metal ion concentration to maximise removal efficiency. FTIR spectroscopy was also employed to identify and confirm functional groups critical for metal ion binding, providing molecular insights into the interaction between metal ions and the biosorbent surface. Comparative analysis of the biosorption capacities of RRP and ATRP was performed, and adsorption behaviour was further characterised using Langmuir and Freundlich isotherm models to elucidate adsorption mechanisms and equilibrium conditions. The Langmuir and Freundlich isotherm models were selected to describe the adsorption behaviour, presenting valuable insights into the adsorption mechanism and surface characteristics of ATRP. Statistical analyses were applied to validate the effectiveness of ATRP in terms of environmental sustainability.

Materials and Methods

Chemicals and instrumentation

Nickel (II) chloride salt ($NiCl_2$), chromium (VI) oxide salt (CrO_3), sodium hydroxide (NaOH), and hydrochloric acid (HCl) were purchased from Merck. All reagents were of analytical grade purity and were used as received, while the pH of the solutions was adjusted using 1M HCl and 1M NaOH. Laboratory-made distilled water and deionised water were the solvents used.

Serial dilution solutions for Cr(VI) and Ni(II) were prepared from an appropriate 1000 mg/L stock solution. All solutions were prepared using deionised water. For this study, Flame Atomic Absorption Spectrophotometry (FAAS) Perkin Elmer Analyst 800 and FTIR Bruker Tensor 27 Spectrometer were used as the main instruments for the heavy metal's determination and chemical characterisation, respectively. Calibration curves were constructed from FAAS using absorbance values versus the analyte concentrations applied, with R^2 = 0.995. Wavelengths used to identify targeted heavy metals were 357.87 nm for Cr and 232.0 nm for Ni.

Preparation of biosorbents

Rambutan peels were sourced from Kampung Lundang Paku in Kota Bharu, Kelantan, a region known for its agricultural abundance. The selection of rambutan peels was driven by their high availability as a waste product, which aligns with the study's environmental goals of waste valorisation and resource efficiency. Rambutan peels were processed into two distinct forms: raw and acid-treated. **Figure 1** illustrates various stages in the preparation of rambutan peels as a biosorbent, showcasing the sequential steps involved in the washing, drying, grinding, sieving, and acid treatment of the raw peels.

The preparation of RRP involved a modification method from Rinaldi et al. and Mohd Sidek et al. by thoroughly washing obtained rambutan peels with deionised water, dried in an oven for 24 hours at 80ºC [33-34]. Upon drying, the dried peels were then milled and sieved with a diameter of 250 µm to 300 µm. The dried peels were then kept in an airtight container for further use. **Figure 2** shows several preparation stages of the rambutan peels as a biosorbent, showing the raw form before washing, after oven drying, and after milling, before sieving to achieve a uniform particle size.

The acid treatment involved immersing the 25 g of dried peels in 150 mL of 1M HCl solution with continuous stirring for 2 hours at 80ºC, followed by neutralisation with NaOH. After the acid treatment, the mixture was then filtered, and the solid residue was washed several times with distilled water to remove any excess acid. The residue was then dried in an oven at 60°C and stored in airtight containers for further use.

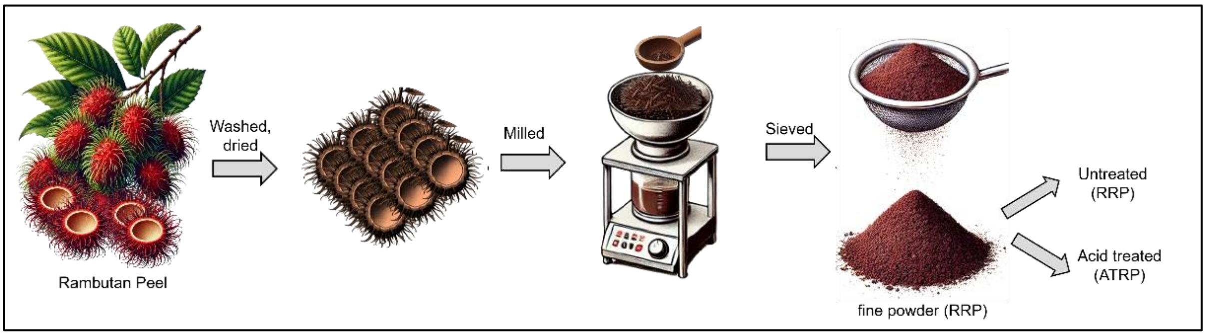

Figure 1. Preparation of biosorbents

A B C

Figure 2. Stages of rambutan peels: (A) before washing, (B) after drying in the oven, and (C) after milling

Characterisation of biosorbents

The chemical characterisation for both RRP and ATRP biosorbents was conducted on the FTIR using the KBr pellet method with a scan range of 400-4000 cm^{-1}. The FTIR spectra of both biosorbents were recorded and compared to identify changes in functional groups induced by acid treatment.

Batch biosorption study

Aqueous solutions of Cr(VI) and Ni(II) were prepared by dissolving their respective salts in deionised water, with concentrations adjusted through serial dilution. Batch biosorption experiments were systematically performed to evaluate the effects of varying contact times (30, 60, 90, 120, and 150 minutes), pH levels (3, 5, 7, 9, and 11), adsorbent dosage (0.5, 1, 2, 3, and 4 g) and metal ion concentration (5, 10, 25, 50, and 100 mg/L) on the removal efficiency of Cr(VI) and Ni(II) ions. 1.0 g of RRP and ATRP were added in two different 250-mL beakers containing 100 mL of a 10 mg/L Ni(II) ion solution. The solution was then stirred at 30°C using a magnetic stirrer before being collected in falcon tubes. The steps were repeated using a Cr(VI) ion solution. The residual metal ion concentrations were quantified using FAAS. The biosorption process was evaluated through the Langmuir and Freundlich isotherms to determine the adsorption characteristics and identify the most suitable model for describing the adsorption equilibrium.

Batch experiments were conducted at a controlled temperature of 30°C with a constant agitation speed of 150 rpm to ensure reproducibility, and the solution pH was adjusted using calibrated pH meters. For all the parameters, the process was replicated three times to get a sample size of N = 15 for each parameter. Blank experiments were conducted to ensure the accuracy and precision of the measurements.

Data analysis

The biosorption capacity, q_e (mg/g), was calculated using the following Eq. 1 [33, 34].

$$q_e = \frac{C_0 - C_e}{m} \times V \quad \text{(Eq. 1)}$$

where C_0 and C_e are the initial and equilibrium concentrations (mg/L), m is the biosorbent weight (g), and V is the volume of the reaction system (L).

Data were analysed using SPSS Statistics 26 and the Mann-Whitney U Test as a non-parametric statistical test to assess significant differences in biosorption capacities between Cr(VI) and Ni(II) under various conditions.

Results and Discussion

Characterisation: FTIR analysis

The chemical characterisation of RRP and ATRP was analysed using FTIR, as illustrated in **Figure 3**. A comparative analysis of the spectra indicates that the ATRP exhibited much higher peak intensities compared to the RRP, indicating modifications in the lignin structure due to acid treatment. Lignin, a complex and highly cross-linked phenolic polymer, presents significant obstacles in biosorption due to its ability to block active sites on cellulose and hemicellulose, thereby limiting the availability of functional groups crucial for metal ion binding. The FTIR analysis focused on detecting key functional groups, including -OH, -COOH, and $-CH_2$, to observe structural changes post-treatment.

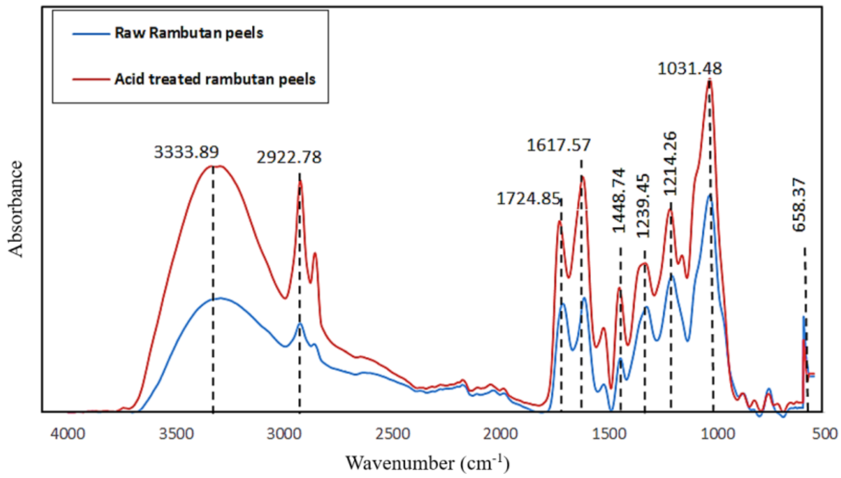

Figure 3. FTIR spectra of rambutan peels before and after treatment with HCl

Figure 3 revealed significant structural changes post-acid treatment, with a marked increase in the intensity of peaks corresponding to -OH and $-CH_2$ groups, highlighting the effects of lignin alterations. Studies have shown that acid treatment can effectively modify lignin structures and increase accessibility to functional groups essential for metal binding [29, 33-34]. Consistent with Hasanah et al., a similar broad peak was observed at 3333.89 cm^{-1}, corresponding to -OH stretching vibrations, and shows a marked increase in intensity in ATRP [35]. This enhancement suggests that the acid treatment has modified the lignin structure, exposing additional -OH groups from cellulose and hemicellulose that were previously shielded by lignin, thereby increasing potential binding sites for metal ions.

Similarly, the peak at 2922.78 cm^{-1}, associated with $-CH_2$ stretching in cellulose, appears more pronounced in ATRP, signifying the structural adjustments occurring in cellulose after acid treatment. The increased intensity of this peak after acid treatment suggests a higher degree of exposure to methylene groups, which are now more accessible due to the partial hydrolysis of surrounding matrix components. Although $-CH_2$ groups themselves do not directly bind metal ions, their exposure enhances the surface area and porosity of the material, thereby improving the accessibility of other functional groups such as -OH and -COOH, which can more effectively participate in metal ion binding.

Notably, the intensified C=O peak at 1724.85 cm^{-1} in ATRP indicates that acid treatment has enhanced the availability of -COOH groups within the modified lignin structures, which is essential for metal binding. The peak at 1617.57 cm^{-1}, attributed to aromatic C=C stretching within the lignin structure, was more pronounced after acid treatment. This suggests that the acid treatment has modified the lignin, likely by depolymerising its complex matrix and exposing more aromatic rings. The exposed aromatic rings facilitate π-cation interactions, a significant mechanism in the adsorption of metal ions as reported by Łojewska et al. [36]. Additionally, these aromatic structures, in conjunction with nearby OH or C=O groups, provide a synergistic effect that enhances the material's affinity for heavy metals by creating a multi-functional adsorption surface [36]. Additionally, the synergistic proximity of these aromatic structures with -OH and C=O groups contribute to a multifunctional adsorption surface, further enhancing biosorption capacity. The enhanced peaks in the fingerprint region, especially the C-O-C stretch at 1031.48 cm^{-1}, suggest improved exposure of polysaccharide groups, contributing to ATRP's superior metal-binding capacity [17-21, 33-35]. The observed prominent peaks, specifically -OH for ATRP compared to RRP, are consistent with similar findings in acid-treated agricultural biosorbents such as modified rice husk, which was reported by Bhatnagar et al. and Rai et al., where the acid treatment enhanced accessibility of functional groups critical for metal ion binding [17-21, 33-35]. These modifications create a more favourable environment for Cr(VI) and Ni(II) biosorption by increasing available binding sites. The structural modification underscores ATRP's potential as an efficient, sustainable biosorbent for heavy metal remediation.

Batch biosorption findings

The optimal biosorption conditions indicated that the most effective adsorbent technique could efficiently remove heavy metals from the aqueous solution. The biosorption analysis of Cr(VI) and Ni(II) was conducted using the batch biosorption method under various parameters. The parameters involved are contact time (30, 60, 90, 120, and 150 minutes) and pH levels (3, 5, 7, 9, and 11), adsorbent dosage (0.5, 1, 2, 3, and 4 g), and metal ion concentration (5, 10, 25, 50, and 100 mg/L).

Effect of contact time

The contact time parameter plays a crucial role in the biosorption process and environmental analysis, as it directly impacts the efficiency of heavy metal removal from wastewater. The effect of contact time on the biosorption of Cr(VI) and Ni(II) by RRP and ATRP was investigated and illustrated in **Figure 4** to determine the optimal duration required for maximum Cr(VI) and Ni(II) ion removal.

As depicted in **Figure 4**, the initial Cr(VI) and Ni(II) ion biosorption rate using both RRP and ATRP was rapid within the first 30 minutes, indicative of the high availability of active sites on the adsorbent surfaces where a large number of binding sites are initially available, allowing for quick uptake of metal ions.

In **Figure 4(A)**, the percentage removal of Cr(VI) by RRP started at 25.93% within the first 30 minutes and gradually increased to 36.8% by 150 minutes, indicating a slower and less efficient biosorption process. ATRP, however, exhibited a much higher initial removal of Cr(VI) at 70.11% within the first 30 minutes, peaking at 76.06% by 120 minutes, and then stabilising around 68-70%. This demonstrates the effectiveness of acid treatment in enhancing biosorption capacity, as it increases the availability of active sites by removing lignin and exposing more functional groups on the cellulose matrix.

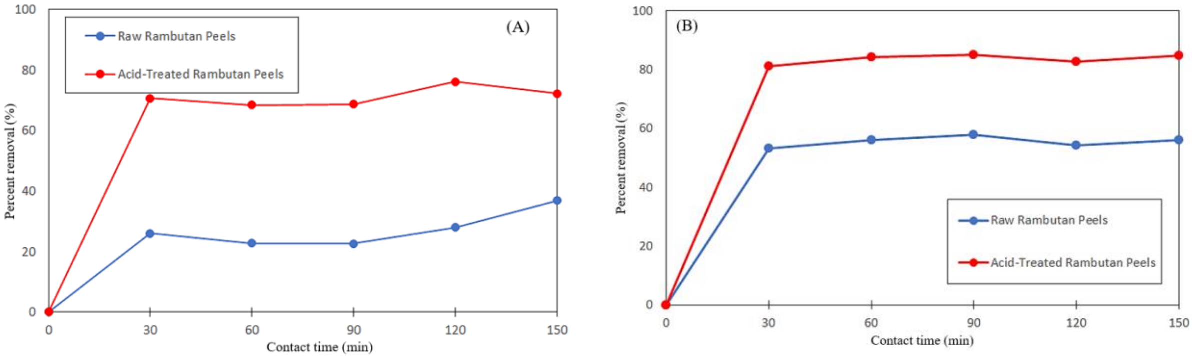

Figure 4. Effect of contact time (30-150 min) on percentage removal of (A) Cr(VI) and (B) Ni(II) using 1.0 g ATRP biosorbents with 10 mg/L initial concentration at pH 7

Similarly, Ni(II) biosorption followed a comparable trend as observed in Figure 4(B), with higher overall removal percentages compared to Cr(VI). The percentage removal of Ni(II) by RRP reached 53.2% within 30 minutes, gradually increasing to a peak value of 57.8% at 90 minutes, beyond which the biosorption rate plateaued, indicating that equilibrium had been achieved. In contrast, ATRP demonstrated a significantly higher biosorption capacity, with an initial removal of 81.16% at 30 minutes, peaking at 88.79% by the 90-minute mark. The biosorption equilibrium for ATRP was maintained with slight fluctuations around 84.73% between 120 and 150 minutes.

The rapid initial uptake, followed by equilibrium, indicates that a contact time of 120 minutes is optimal for Cr(VI) removal, while 90 minutes is sufficient for Ni(II) removal. Efficient management of contact time not only maximises the biosorption capacity but also enhances the overall performance of downstream processes in wastewater treatment, ensuring compliance with environmental regulations. Therefore, understanding and optimising contact time is essential for achieving effective and efficient biosorption in environmental applications [27-29].

The findings demonstrate that ATRP significantly outperforms RRP in the biosorption of both Cr(VI) and Ni(II), highlighting the effectiveness of acid treatment in optimising the biosorption process. The enhanced biosorption performance of ATRP compared to RRP can be attributed to the role of acid modification, which effectively disrupts lignin's structure, thereby exposing more active sites for Cr(VI) and Ni(II) ion binding. This is a similar indication of successful chemical activation, which has successfully modified the lignin and released a more active surface of the cellulose for rambutan peels for efficient heavy metal sorption [33, 34]. Given the superior performance of ATRP, this study identifies ATRP as the more effective biosorbent for further pH optimisation rather than RRP.

Effect of pH

The pH of the solution is a critical parameter in the biosorption process, profoundly influencing the biosorption efficiency of heavy metals from aqueous solutions. As illustrated in **Figure 5**, the effect of pH on Cr(VI) and Ni(II) removal by ATRP was systematically evaluated, demonstrating that pH plays a pivotal role in determining the biosorption capacity of the biosorbent.

For Cr(VI), the biosorption efficiency was maximised at pH 5, with 76.06% of Cr(VI) ions effectively removed from the solution, as shown in **Figure 5**. In aqueous solutions, Cr(VI) exists as negatively charged oxyanions, primarily as chromate (CrO_4^{2-}) under alkaline conditions and dichromate ($Cr_2O_7^{2-}$) in acidic conditions. This negative charge allows Cr(VI) to interact with positively charged functional groups on the ATRP surface, such as protonated OH groups, facilitating effective biosorption through electrostatic attraction [36]. As the pH increases beyond 5, the biosorption efficiency declines, particularly at pH 11, where only 28.90% removal was observed. This reduction can be attributed to increased competition from hydroxide ions at higher pH levels, which inhibit Cr(VI) biosorption by occupying active sites on the adsorbent. Conversely, at pH 3, the removal efficiency was also lower with 54.6% removal, which may be due to the reduction of Cr(VI) to Cr(III) under highly acidic conditions, which has a lower affinity for ATRP [28, 29, 37].

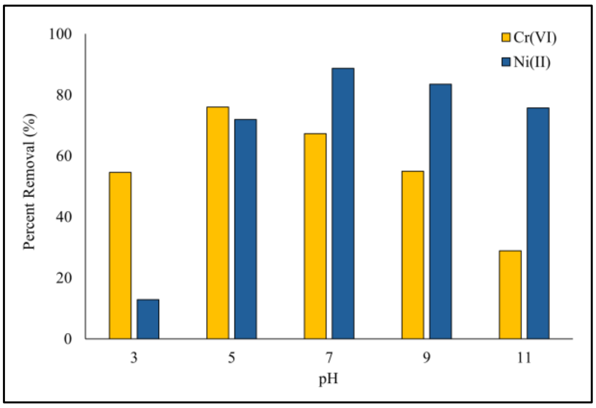

Figure 5. Effect of pH (3-11) on percentage removal of 10 mg/L initial concentration of Cr(VI) and Ni(II) using 1.0 g ATRP biosorbent

Meanwhile, the optimal pH for Ni(II) biosorption was found to be 7, removing 88.79% of Ni(II) ions, as illustrated in **Figure 5.** This indicates that at neutral pH, the functional groups on the ATRP are most effective in binding Ni(II) ions, likely due to the reduced competition from hydrogen ions (H^+), which are more prevalent at lower pH levels. At pH 3, the biosorption efficiency decreased significantly to 12.87%, highlighting the competitive inhibition by H^+ ions, which reduces the availability of active sites for Ni(II) binding. At higher pH levels of pH 9 and 11, the biosorption efficiency remained relatively high, though slightly diminished compared to pH 7. This reduction can be explained by the decreased solubility of Ni(II) at alkaline pH, which limits the number of free Ni(II) ions available for biosorption [24, 38, 39].

At alkaline conditions, the increase in turbidity of metal ions was observed, as shown in **Figure 6**, by the bulky appearance of the aqueous solution before adding the biosorbent. This turbidity suggests that metal ion precipitation occurs at higher pH values, indicating that biosorption results at these pH values should be interpreted with caution, as both precipitation and adsorption could contribute to the overall removal [15, 23, 29, 38].

Effect of adsorbent dosage

Optimising dosage is crucial to maximising removal efficiency and cost-effectiveness, as excessive adsorbent use adds minimal benefit while increasing operational costs. The effect of adsorbent dosage on the biosorption efficiency of Cr(VI) and Ni(II) was evaluated and illustrated in **Figure 7**. Identifying an optimal dosage is crucial, as it maximises biosorption efficiency while maintaining cost-effectiveness. Excessive adsorbent quantities may not improve removal performance and can increase operational costs, particularly in large-scale applications. Therefore, fine-tuning the ATRP dosage is essential to achieving an optimal balance between biosorption performance and economic feasibility, rendering ATRP a practical and sustainable option for industrial-scale wastewater treatment.

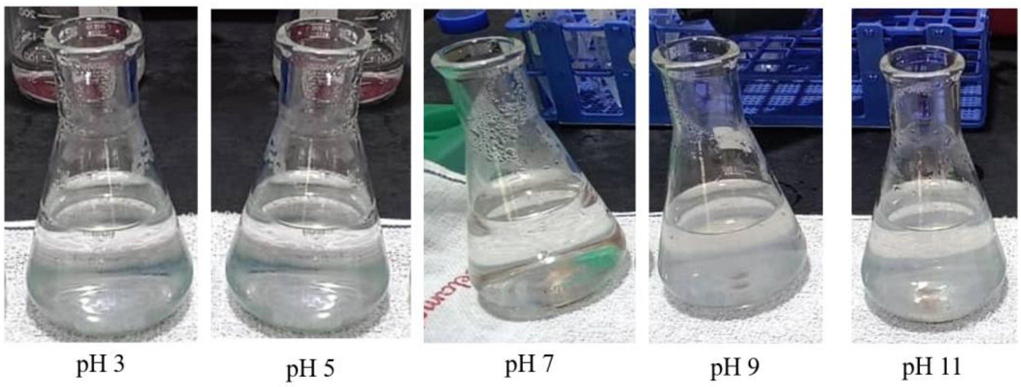

Figure 6. Visual observations of metal ion solutions at varying pH levels before biosorbent addition

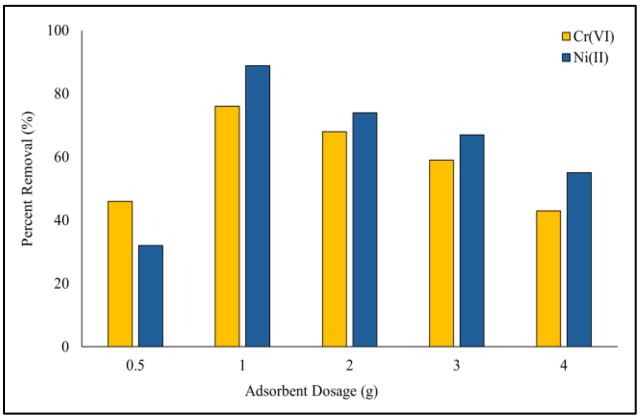

Figure 7. Effect of adsorbent dosage (0.5-4 g) on the removal of a fixed 10 mg/L initial concentration of Cr(VI) and Ni(II) at pH 5 and pH 7, respectively

As illustrated in **Figure 7**, increasing the adsorbent dosage initially enhances removal efficiencies, with maximum biosorption observed at 1 g for both metals, with 76.06% for Cr(VI) and 88.79% for Ni(II). This improvement is attributed to the increased availability of active adsorption sites and surface area, which facilitate more extensive interactions between metal ions and the ATRP surface. However, as the dosage exceeds 1 g, the removal efficiency declines, with Cr(VI) and Ni(II) removal decreasing to 38.1% and 48.3%, respectively, at a 4 g dosage.

This decline can be attributed to the aggregation of ATRP particles at higher dosages, which leads to overlapping active sites and limits the effective surface area exposed to metal ions. Furthermore, the high dosage of adsorbent can create a saturation effect, where a large proportion of the adsorbent's surface remains unsaturated due to insufficient availability of metal ions. This phenomenon results in a decrease in the biosorption capacity per unit mass as excess adsorbent particles compete for limited ion availability, thereby reducing efficiency [24-39].

Effect of initial concentration

The initial concentration of metal ions plays a critical role in defining the adsorption capacity of ATRP, as shown in **Figure 8**. The effect of varying initial concentrations (5–100 mg/L) on the removal efficiency of Cr(VI) and Ni(II) was evaluated under optimised conditions. The maximum removal efficiencies were achieved at a concentration of 10 mg/L, with Cr(VI) removal at 76.06% and Ni(II) at 88.79%. At this concentration, the availability of active adsorption sites on ATRP is sufficient to accommodate the metal ions, enabling high biosorption efficiency.

However, as the initial concentration increases beyond 10 mg/L, a decline in removal efficiency is observed, with Cr(VI) and Ni(II) removal decreasing to 28.2% and 34.5%, respectively, at 100 mg/L. This reduction can be attributed to the saturation of active sites on the ATRP surface as the concentration of metal ions increases, leading to increased competition among ions for available sites. Consequently, as metal ion content rises, the adsorption capacity of the adsorbent reaches a limit, resulting in reduced removal efficiency. Similar trends have been observed with corncob, as reported by Chaudhari and Patkar, where increasing metal ion concentration leads to saturation of adsorption sites and diminished removal rates [40].

This suggests that ATRP is most effective at moderate concentrations, and adjustments to adsorbent dosage or extended contact times may be necessary to maintain high adsorption performance at elevated concentrations. These findings underscore the importance of optimising initial concentration to balance adsorption efficiency and maximise the potential of ATRP in practical applications.

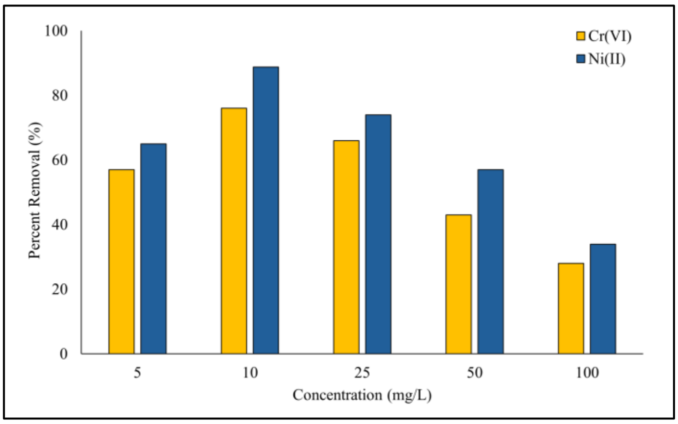

Figure 8. Effect of initial concentration (5–100 mg/L) on the removal of Cr(VI) at pH 5 and Ni(II) at pH 7 using 1.0 g of biosorbent

Adsorption isotherms

Adsorption isotherm analysis allows for the characterisation of the adsorbate distribution between the solid and liquid phases at equilibrium, providing insights into the adsorption mechanism. This study employed the Langmuir and Freundlich isotherm models, as illustrated in **Figures 9A** and **9B**, respectively, to evaluate the adsorption of Cr(VI) and Ni(II) onto ATRP at equilibrium [33, 34, 40].

Langmuir isotherm

The Langmuir model assumes monolayer adsorption on a homogeneous surface, with all active sites having equal affinity for the adsorbate. The linear form of the Langmuir isotherm was expressed as Eq. 2 [39, 40].

$$\frac{1}{q_e} = \frac{1}{q_m K_L C_e} + \frac{1}{q_m} \quad \text{(Eq. 2)}$$

where q_m denotes the maximum adsorbent's monolayer capacity for the adsorbate (mg/g) and K_L signifies the constant of the Langmuir equilibrium related to the Cr(VI) and Ni(II) adsorption binding energy (L/mg).

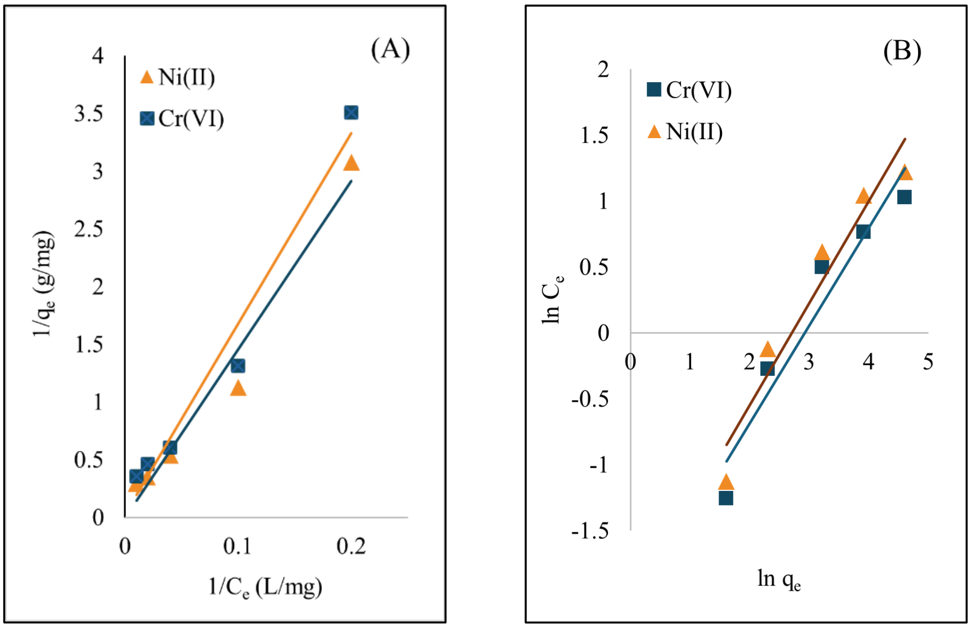

Figure 9. Adsorption isotherms (A) Langmuir and (B) Freundlich of Cr(VI) and Ni(II) onto ATRP

Figure 9A shows linear correlation plots between C_e/q_e and C_e. Langmuir constants such as q_m and K_L are determined from the slope and intercept of the plot. The R^2 values of correlation coefficients were utilised to find the best-fit linear equation [27]. The q_m for Cr(VI) and Ni(II) was 33.4448 mg/g and 416.6667 mg/g, with K_L of 0.0018 L/mg and 0.0002 L/mg, respectively. The high correlation coefficients for Cr(VI) (R^2=0.9698) and Ni(II) (R^2=0.9699) suggest the best fitting of the experimental data to the Langmuir isotherm, indicating favourable monolayer adsorption.

The shape of the Langmuir isotherm can be evaluated using the dimensionless separation factor (R_L) to determine the more favourable isotherm. R_L was estimated using Eq. 3 [40, 41].

$$R_L = \frac{1}{1 + C_0 K_L} \quad \text{(Eq. 3)}$$

The value of R_L specifies the isotherm shape; it is irreversible when $R_L = 0$, favourable when $0 < R_L < 1$, linear when $R_L = 1$, and unfavourable when $R_L > 1$. The R_L value was found to be 0.9822 for Cr(VI) and 0.9984 for Ni(II), demonstrating that the ATRP biosorbent is well-suited for effective heavy metal removal under the optimised conditions, as R_L values close to zero indicate a highly favourable adsorption process.

Freundlich isotherm

Freundlich isotherm assumes multilayer adsorption, and the adsorbent is considered to have a heterogeneous surface energy system that is satisfactory for low adsorptive concentrations [40, 41]. The Freundlich isotherm was estimated using Eq. 4.

$$\ln q_e = \ln K_F + (1/n) \ln C_e \quad \text{(Eq. 4)}$$

The Freundlich isotherm constants are represented by K_F and *n*. K_F is the distribution or adsorption coefficient and indicates the adsorption capacity of the adsorbent. Figure 9B shows that the plot of log q_e versus log C_e represents a straight line with a slope value of 1/*n*.

The Freundlich constants K_F and 1/*n* were computed using Eq. 4. This model, which assumes adsorption on a heterogeneous surface, yielded a K_F of 0.1143 for Cr(VI) and 0.1230 for Ni(II). The values of *n*, which are 1.3479 for Cr(VI) and 1.2910 for Ni(II), indicate favourable adsorption when *n* is greater than 1. However, the lower R^2 values (R^2 = 0.9296 for Cr(VI) and R^2 = 0.9368 for Ni(II)) indicate that the Freundlich model provides a less accurate fit compared to the Langmuir model, suggesting that monolayer adsorption is more dominant in this system.

Table 1 summarises the key isotherm parameters, with Langmuir constants q_m of 33.4448 mg/g for Cr(VI) and 416.6667 mg/g for Ni(II), which are notably higher than those of other biosorbents like date palm leaves and almond husks, which have exhibited capacities of approximately 22.47 mg/g for Cr(VI) and 37.175 mg/g for Ni(II), confirming ATRP's competitive efficacy [38, 41]. The R_L values for Cr(VI) and Ni(II), 0.9822 and 0.9984, respectively, indicate favourable adsorption, demonstrating ATRP's suitability for efficient metal ion removal under optimised conditions.

This analysis indicates that the Langmuir model more accurately describes the adsorption behaviour of Cr(VI) and Ni(II) on ATRP, suggesting a monolayer adsorption process with favourable characteristics [33, 34, 40, 43]. The higher R^2 values of the Langmuir model (R^2 = 0.9698 for Cr(VI) and R^2 = 0.9699 for Ni(II)) compared to the Freundlich model underscore the better fit to a monolayer adsorption mechanism.

Table 1. Adsorption isotherms

Langmuir			**Freundlich**		
Parameters	**Cr(VI)**	**Ni(II)**	**Parameters**	**Cr(VI)**	**Ni(II)**
q_m (g/mg)	33.4448	416.6667	K_F	0.1143	0.1230
K_L (L/mg)	0.0018	0.0002	*n*	1.3479	1.2910
R^2	0.9698	0.9699	R^2	0.9296	0.9368
R_L	0.9822	0.9984			

Mean difference between percent removal of Ni(II) and Cr(VI) adsorbed by RRP and ATRP biosorbents

The biosorption capacities of RRP and ATRP for Cr(VI) and Ni(II) were evaluated using the Mann-Whitney U test. The Mann-Whitney U test was utilised to compare biosorption efficiencies between RRP and ATRP under non-normal data distributions, ensuring statistically robust results without parametric assumptions. **Table 2** summarises the results of the statistical analysis, showing the mean percentage removal, IQR, and statistical significance of the differences between RRP and ATRP.

Table 2. The mean difference between percent removal of Ni(II) and Cr(VI) using RRP and ATRP

	Cr(VI)		**Ni(II)**	
	RRP	**ATRP**	**RRP**	**ATRP**
N	15	15	15	15
Mean (IQR) % removal	28 (6)	54 (35)	58 (20)	64 (10)
Z statistic	-3.629		-2.220	
p value[a]	0.009[a]		0.026[a]	

[a] Mann-Whitney test

ATRP demonstrated significantly higher biosorption efficiencies compared to RRP for both metals. Specifically, ATRP achieved a mean Cr(VI) removal of 54%, compared to 28% for RRP, with a Z statistic of -3.629 and a p-value of 0.009 (p <0.05). Similarly, for Ni(II), ATRP showed a mean removal efficiency of 64%, compared to 58% for RRP, with a Z statistic of -2.220 and a p-value of 0.026 (p <0.05). The null hypothesis for both Cr(VI) and Ni(II) was rejected, confirming a significant mean difference in Cr(VI) and Ni(II) removal between both biosorbents, in which ATRP significantly outperformed RRP in metal biosorption.

The enhanced performance of ATRP can be attributed to the acid treatment, which effectively removes lignin and enhances more active sites and functional groups, such as -OH and -COOH groups, that are critical for metal ion binding. The statistical significance of the differences between RRP and ATRP underscores the importance of chemical modification in improving the efficacy of biosorbents derived from agricultural waste, which also provides a robust basis for the application of ATRP in environmental remediation [33-28].

Conclusion

This study demonstrates that ATRP is a highly effective biosorbent for removing Cr(VI) and Ni(II) from aqueous solutions, significantly outperforming RRP. The batch biosorption experiments revealed that ATRP achieved maximum removal efficiencies of 76.06% for Cr(VI) at pH 5 with a contact time of 120 minutes and 88.79% for Ni(II) at pH 7 with a contact time of 90 minutes. In comparison, RRP showed lower efficiencies, with 36.8% for Cr(VI) and 57.8% for Ni(II) under similar conditions. These findings emphasise the importance of acid treatment in lignin modification, thereby exposing additional active sites by enhancing the availability of -OH and $-CH_2$ groups, which play a key role in metal ion binding. For ATRP, the R^2 values of the Langmuir isotherm model were 0.9698 and 0.9699 with R_L values of 0.9822 and 0.9984 for both Cr(VI) and Ni(II), respectively, revealing the best fitting of the experimental data to the Langmuir than the Freundlich isotherm. Using the Mann-Whitney U test to do statistical analysis confirmed that there are significant differences between ATRP and RRP in their biosorption capacities. This shows that ATRP could be a cost-effective and long-lasting way to treat industrial wastewater. These results directly support the objectives of SDG6, SDG12, and SDG14 by promoting innovative, sustainable solutions for wastewater pollution control.

Given the promising results, future research should explore the feasibility of ATRP for large-scale industrial applications and investigate combinations with other biosorbents to enhance efficiency. Additionally, synergistic combinations of rambutan peels with other agricultural wastes or modifications with magnetism or polymeric compounds could broaden the potential of biosorbents in environmental remediation. [44-46].

Challenges such as the regeneration of biosorbents, potential costs, and the handling of large volumes of wastewater also need to be addressed to ensure the feasibility of ATRP in real-world applications. While ATRP shows promising reusability, the regeneration efficiency may decrease over repeated cycles, warranting further study to optimise regeneration protocols for potential industrial applications. For sustainable use and disposal of the ATRP biosorbent, a cradle-to-grave management approach is recommended. The spent biosorbent can be regenerated using mild desorbing agents such as dilute HCl or NaCl, which effectively desorb Cr(VI) and Ni(II) ions, allowing the ATRP to be reused across multiple cycles with minimal degradation. After multiple cycles, when biosorption efficiency declines, safe disposal is essential [18, 47]. For final disposal, spent ATRP could undergo stabilisation or controlled thermal treatment to immobilise bound metals, minimising environmental impact and leaching risks in landfill conditions [48]. This holistic approach not only enhances the economic and environmental feasibility of ATRP but also aligns with sustainable waste management practices, underscoring its potential as a viable biosorbent for heavy metal remediation.

Acknowledgement

The authors gratefully acknowledge Universiti Sains Malaysia (USM), Kubang Kerian, Kelantan, Malaysia, for providing essential support and research facilities.

References

1. Xia, Y., Li, Y., and Xu, Y. (2022). Adsorption of Pb(II) and Cr(VI) from aqueous solution by synthetic allophane suspension: Isotherm, Kinetics, and Mechanisms. *Toxics*, 10(6): 291.
2. Dass, M. V. (2024b, February 27). Sungai Kim Kim, 3 lagi tercemar di Pasir Gudang. Harian Metro. Access from https://www.hmetro.com.my/mutakhir/ 2024/02/ 1064742/sungai-kim-kim-3-lagi-tercemar-di-pasir-gudang
3. Dass, M. V. (2023b, October 28). 14 sungai di Johor dikategorikan paling tercemar. Harian Metro. Access from https://www.hmetro.com.my/mutakhir/2023/10/1024676/14-sungai-di-johor-dikategorikan-paling-tercemar
4. Ibrahim, M. I. (2024b, June 6). 25 sungai di Malaysia tercemar kelas 3 dan 4. Berita Harian. Access from https://www.bharian.com.my/berita/nasional/2024/06/1255563/25-sungai-di-malaysia-tercemar-kelas-3-dan-4
5. Selvaraju, A., Abdul Halim, A. N. S., and Abdul Keyon, A. S. (2020). Determination of selected heavy metal concentrations in unregistered face whitening creams sold in Johor Bahru, Johor, Malaysia by using inductively coupled plasma optical emission spectroscopy and their health risk assessment. *Malaysian Journal of Analytical Sciences*, 24(5): 670-681.
6. Arzoo, A., and Satapathy, K. B. (2017). A review on sources of heavy metal pollution and its impacts on environment. *International Journal of Current Advanced Research*, 6(12): 8098-8102.
7. Balogun, K. J. (2021). Risk Assessment of Trace Metal Intake through Consumption of Four Fish Species from Upper Region of Barrier Lagoon Coast Waters, Southwest, Nigeria. *Journal of Environment Pollution and Human Health*, 9(1): 16-21.
8. Mat Ripin, S. N., Hasan, S., Kamal, M. L., and Mohd Hashim, N. (2014). Analysis and pollution assessment of heavy metal in soil, Perlis. *Malaysian Journal of Analytical Sciences*, 18(1): 155-161.
9. Guidelines for drinking-water quality: fourth edition incorporating the first and second addenda. (2022b, March 21). https://www.who.int/publications/i/item/9789240045064
10. National Primary Drinking Water Regulations | US EPA. (2024c, August 23). US EPA. Access from https://www.epa.gov/ground-water-and-drinking-water/national-primary-drinking-water-regulations
11. Abegunde, S. M., Idowu, K. S., Adejuwon, O. M., and Adeyemi-Adejolu, T. (2020b). A review on the influence of chemical modification on the performance of adsorbents. *Resources Environment and Sustainability*, 1: 100001.
12. Vasić, K., Primožič, M., Knez, Ž., Leitgeb, M. (2023). Efficient removal of Cr(VI) ions from aqueous solutions using arabinogalactan coated magnetic nanoparticles. *Chemical Engineering Transactions*. 99: 205-210.
13. Yaashikaa P. R., Palanivelu J., and Hemavathy R.V. (2024). Sustainable approaches for removing toxic heavy metal from contaminated water: a comprehensive review of bioremediation and biosorption techniques. *Chemosphere*, 357:141933.
14. Hussain, M. K., Khatoon, S., Nizami, G., Fatma, U. K., Ali, M., Singh, B., Quraishi, A., Assiri, M. A., Ahamad, S., and Saquib, M. (2024). Unleashing the power of bio-adsorbents: efficient heavy metal removal for sustainable water purification. *Journal of Water Process Engineering*, 64: 105705.
15. Jena, P. S., Pradhan, A., Nanda, S. P., Dash, A. K., and Naik, B. (2022). Biosorption of heavy metals from wastewater using saccharomyces cerevisiae as a biosorbent: a mini review. *Materials Today Proceedings*, 67: 1140-1146.
16. THE 17 GOALS | Sustainable Development. (n.d.-c). https://sdgs.un.org/goals
17. Zhang, Z., Chen, Y., Wang, D., Yu, D., & Wu, C. (2023b). Lignin-based adsorbents for heavy metals. *Industrial Crops and Products,* 193: 116119.
18. Bhatnagar, A., Sillanpää, M., and Witek-Krowiak, A. (2015). Agricultural waste peels as versatile biomass for water purification – a review. *Chemical Engineering Journal*. 270: 244-271.
19. Elgarahy, A., Elwakeel, K., Mohammad, S., and Elshoubaky, G. (2021). A critical review of biosorption of dyes, heavy metals and metalloids from wastewater as an efficient and green process. *Cleaner Engineering and Technology,* 4: 100209.
20. Aschale, M., Tsegaye, F., and Amde, M. (2021c) Potato peels as promising low-cost adsorbent for the removal of lead, cadmium, chromium and copper from wastewater. *Desalination And Water Treatment.* 222: 405-415.
21. Chong, Z. T., Soh, L. S., and Yong, W. F. (2023). Valorization of agriculture wastes as biosorbents for adsorption of emerging pollutants:

Modification, remediation and industry application. *Results in Engineering*. 17: 100960.

22. Marpongahtun, N., Andriayani, N., Muis, Y., Gea, S., Amaturrahim, S. A., Attaurrazaq, B., Daulay, A., and Salmiati, S. (2024b). Biomass-derived N-doped carbon dots/TiO_2 for visible-light-induced degradation of methyl orange in wastewater. *Chemistry Africa*, 24: 970.
23. El-Maghraby, L. M. (2019). Removal of copper (II) and ferric (III) ions from aqueous solutions by adsorption using potato peel. *Assiut Journal of Agricultural Sciences/Assuit Journal of Agricultural Sciences*, 50(3): 98-111.
24. Hidayah, N., Putri, V. D., Elma, M., Mahmud, N., Syauqiah, I., Amenia, A., Putra, D. G. L., Akbar, H. R., and Rahma, A. (2022). The functionalization of pyrolyzed palm empty fruit bunches-based membranes adsorbent by fourier-transform infrared spectroscopy. *IOP Conference Series Materials Science and Engineering*, 1212(1): 012026.
25. Dey, S., Veerendra, G. T. N., Padavala, S. S. A. B., and Manoj, A. V. P. (2023). Evaluate the use of flower waste biosorbents for treatment of contaminated water. *Water-Energy Nexus*. 6:187-223.
26. Li, W., Chai, L., Du, B., Chen, X., and Sun, R. C. (2023). Full-lignin-based adsorbent for removal of Cr(VI) from waste water. *Separation and Purification Technology*. 306: 122644.
27. Inoue, K., Parajuli, D., Ghimire, K., Biswas, B., Kawakita, H., Oshima, T., and Ohto, K. (2017). Biosorbents for removing hazardous metals and metalloids. *Materials*, 10(8): 857.
28. Vishvkarma, T., Sharma, A., and Sharma, S. (2017). Adsorption of chromium ion by using neem bark adsorbent. *International Journal of Chemical Studies*. 1325-1327.
29. Rai, R., Aryal, R. L., Paudyal, H., Gautam, S. K., Ghimire, K. N., Pokhrel, M. R., and Poudel, B. R. (2023). Acid-treated pomegranate peel; an efficient biosorbent for the excision of hexavalent chromium from wastewater. *Heliyon*. 9(5): e15698.
30. Jabatan Pertanian Malaysia & Department of Agriculture. (2022). Statistik Tanaman Buah – Buahan. In Fruit Crop Statistics Report. Jabatan Pertanian. http://www.doa.gov.my/
31. Kong, F. C., Adzahan, N. M., Karim, R., Rukayadi, Y., and Ghazali, H. M. (2018). Selected Physicochemical properties of registered clones and wild types rambutan (*Nephelium lappaceum* L.) fruits and their potentials in food products. *Sains Malaysiana,* 47(07): 1483-1490.
32. Phuong, N. N. M., Le, T. T., Dang, M. Q., Van Camp, J., and Raes, K. (2020). Selection of extraction conditions of phenolic compounds from rambutan (*Nephelium lappaceum* L.) peel. *Food and Bioproducts Processing,* 122: 222-229.
33. Rinaldi, R., Yasdi, Y., and Hutagalung, W. L. C. (2018). Removal of Ni(II) and Cu (II) ions from aqueous solution using rambutan fruit peels (*Nephelium Lappaceum* L.) as adsorbent. *AIP Conference Proceedings,* 2018: 5065058
34. Mohd Sidek, N., Syed Draman, S. F., and Mohd, N. (2017). Removal of copper (II) ions from aqueous solution using *Nephelium lappaceum* L. as lignocellulosic biosorbent. *ARPN Journal of Engineering and Applied Sciences.* 10: 3255-3256.
35. Hasanah, M., Juleanti, N., Priambodo, A., Arsyad, F., Lesbani, A., and Mohadi, R. (2022). Utilization of rambutan peel as s potential adsorbent for the adsorption of malachite green, procion red, and congo red dyes. *Ecological Engineering & Environmental Technology,* 23(3): 148-157.
36. Łojewska, J., Miśkowiec, P., Łojewski, T., and Proniewicz, L. (2005). Cellulose oxidative and hydrolytic degradation: In situ FTIR approach. *Polymer Degradation and Stability,* 88(3): 512-520.
37. Fenti, A., Chianese, S., Iovino, P., Musmarra, D., and Salvestrini, S. (2020). Cr(VI) sorption from aqueous solution: a review. *Applied Sciences,* 10(18): 6477.
38. Hasar, H. (2003). Adsorption of nickel(II) from aqueous solution onto activated carbon prepared from almond husk. *Journal of Hazardous Materials,* 97(1-3): 49-57.
39. Islam, M. A., Awual, M. R., and Angove, M. J. (2019). A review on nickel(II) adsorption in single and binary component systems and future path. *Journal of Environmental Chemical Engineering,* 7(5): 103305.
40. Chaudhari, V., and Patkar, M. (2021). Removal of nickel from aqueous solution by using corncob as adsorbent. *Materials Today Proceedings,* 61: 307-314.
41. Chung, J., Sharma, N., Kim, M., and Yun, K. (2022). Activated carbon derived from sucrose and melamine as low-cost adsorbent with fast adsorption rate for removal of methylene blue in wastewaters. *Journal of Water Process Engineering,* 47: 102763.
42. Fawzy, M., Nasr, M., Abdel-Gaber, A., and Fadly, S. (2015). Biosorption of Cr(VI) from aqueous solution using agricultural wastes, with artificial intelligence approach. *Separation Science and Technology,* 51(3): 416-426.
43. Akpomie, K. G., and Conradie, J. (2020). Banana peel as a biosorbent for the decontamination of water pollutants. A review. *Environmental Chemistry Letters,* 18(4): 1085-

1112.
44. Osman, A. I., El-Monaem, E. M. A., Elgarahy, A. M., Aniagor, C. O., Hosny, M., Farghali, M., Rashad, E., Ejimofor, M. I., López-Maldonado, E. A., Ihara, I., Yap, P. S., Rooney, D. W., and Eltaweil, A. S. (2023). Methods to prepare biosorbents and magnetic sorbents for water treatment: a review. *Environmental Chemistry Letters,* 21(4): 2337-2398.
45. Yuan, X., Li, J., Luo, L., Zhong, Z., and Xie, X. (2023). Advances in sorptive removal of hexavalent chromium (Cr(VI)) in aqueous solutions using polymeric materials. *Polymers*. 15(2): 388.
46. Masuku, M., Nure, J. F., Atagana, H. I., Hlongwa, N., and Nkambule, T. T. (2024b). Advancing the development of nanocomposite adsorbent through zinc-doped nickel ferrite-pinecone biochar for removal of chromium (VI) from wastewater. *The Science of the Total Environment*. 908: 168136.
47. Mohan, K. M., and Gajalakshmi, S. (2024). Biosorption for wastewater treatment and post-sorption utilization of treated wastewater and spent biosorbent. *Biological and Hybrid Wastewater Treatment Technology*. Springer pp. 57–90.
48. Ajorloo, M., Ghodrat, M., Scott, J., and Strezov, V. (2022). Heavy metals removal/stabilization from municipal solid waste incineration fly ash: a review and recent trends. *Journal of Material Cycles and Waste Management,* 24(5): 1693-1717.